A Chemical Acetylation based Mass Spectrometry Platform for Histone Methylation Profiling

Francesca Zappacosta[1], Craig D. Wagner[1], Anthony Della Pietra III[2], Sarah V. Gerhart[2], Chad J. Quinn[1], Olena Barbash[2], Michael T. McCabe[2] and Roland S. Annan[1]

Supplemental Material

Table S1: Modified forms of the H4 N-terminal sequence 1-20, SGRGKGGKGLGKGGAKRHRK identified in a top-down experiment [14].

Table S2: Different modified forms of the H4 peptides 1-17 and 4-17 identified after histone propionylation of nuclear extracts from Z-138 cells

Table S3. H3K27 isoforms identified after propionylation of a nuclear extract from KARPAS-422 cells.

Figure S1. Reverse phase chromatography of histone tryptic peptides after acetylation or propionylation

Figure S2. Acetylation and tryptic digestion of a 1:1:0.5:0.5 mixture of Histone H4R3 0MA:MMA:DMA synthetic peptide standards.

Figure S3: Optimization of the Normalized Collision Energy (NCE) for ADMA and SDMA neutral loss from H4R3 1-17 ADMA and SDMA peptides.

Figure S4: Discrimination of H4R3me2 ADMA from SDMA on the histone H4 1-17 peptide by tandem mass spectrometry.

Figure S5. Tandem MS spectra representing species used in Figure 5. H4R3 zero, mono and dimethylarginine and H4R3 ADMA and SDMA.

Figure S6. Extracted ion chromatograms and tandem MS spectra from m/z 726.9178, the $[M+2H]^{2+}$ precursor ion for the tryptic peptide H4 (4-17) + me1.

Figure S7. Tandem MS spectra for H3K27 isoforms represented in Figure 7.

Table S1: Modified forms of the H4 N-terminal sequence 1-20, SGRGKGGKGLGKGGAKRHRK identified in a top-down experiment [14]. After chemical acetylation, the 68 differently modified forms collapse into six.

H4 N-terminal tail forms reported in ref (14)								H4 Isoforms following in-vitro lysine acetylation							
N-terminus	R3	K5	K8	K12	K16	K20	Methyl Units	N-terminus	R3	K5	K8	K12	K16	K20	Methyl Units
ac							0								
ac		ac					0								
ac			ac				0								
ac				ac			0								
ac					ac		0								
ac		ac	ac				0								
ac		ac			ac		0	ac		ac	ac	ac	ac		0
ac			ac		ac		0								
ac				ac	ac		0								
ac		ac	ac	ac			0								
ac		ac	ac		ac		0								
ac		ac		ac	ac		0								
ac			ac	ac	ac		0								
ac		ac	ac	ac	ac		0								
						me1	1								
ac						me1	1								
ac		ac				me1	1								
ac					ac	me1	1								
ac		ac	ac			me1	1								
ac		ac			ac	me1	1								
ac			ac		ac	me1	1	ac		ac	ac	ac	ac	me	1
ac				ac	ac	me1	1								
ac		ac	ac	ac		me1	1								
ac		ac	ac		ac	me1	1								
ac		ac		ac	ac	me1	1								
ac			ac	ac	ac	me1	1								
ac		ac	ac	ac	ac	me1	1								
						me2	2								
ac						me2	2								
ac		ac				me2	2								
ac			ac			me2	2								
ac				ac		me2	2								
ac					ac	me2	2								
ac		ac	ac			me2	2								
ac		ac			ac	me2	2	ac		ac	ac	ac	ac	me2	2
ac			ac		ac	me2	2								
ac				ac	ac	me2	2								
ac			ac	ac		me2	2								
ac		ac	ac	ac		me2	2								
ac		ac	ac		ac	me2	2								
ac		ac		ac	ac	me2	2								
ac			ac	ac	ac	me2	2								
ac		ac	ac	ac	ac	me2	2								
ac						me3	3								
ac		ac				me3	3								
ac			ac			me3	3								
ac				ac		me3	3								
ac					ac	me3	3								
ac		ac	ac			me3	3	ac		ac	ac	ac	ac	me3	3
ac				ac	ac	me3	3								
ac		ac	ac	ac		me3	3								
ac		ac	ac		ac	me3	3								
ac		ac		ac	ac	me3	3								
ac			ac	ac	ac	me3	3								
ac		ac	ac	ac	ac	me3	3								
ac	me1					me2	3								
ac	me1	ac				me2	3								
ac	me1		ac			me2	3								
ac	me1			ac		me2	3								
ac	me1				ac	me2	3								
ac	me1	ac	ac			me2	3	ac	me1	ac	ac	ac	ac	me2	3
ac	me1	ac	ac	ac		me2	3								
ac	me1	ac	ac		ac	me2	3								
ac	me1	ac		ac	ac	me2	3								
ac	me1		ac	ac	ac	me2	3								
ac	me1			ac	ac	me2	3								
ac	me1	ac	ac	ac	ac	me2	3								
ac	me2				ac	me2	4	ac	me2	ac	ac	ac	ac	me2	4

Table S2: Different modified forms of the H4 peptides 1-17 and 4-17 identified by data-dependent and validated by target PRM methods after histone propionylation of nuclear extracts from Z-138 cells. Some of the identifications reported in table 3 are not reported here as they did not meet the stringent validation criteria used for site identification.

H4 Peptide 1-17 SGRGKGGKGLGKGGAKR

N-term	R3	K5	K8	K12	K16	R17	Acetyl Units	Methyl Units
ac	me1	ac		ac	ac		4	1
ac				ac	ac		3	0
ac					ac		2	0
ac	me1				ac		2	1
ac							1	0
ac	me1						1	1

H4 Peptide 4-17 GKGGKGLGKGGAKR

N-term	R3	K5	K8	K12	K16	R17	Acetyl Units	Methyl Units
		ac	ac	ac	ac		4	0
		ac		ac	ac		3	0
			ac	ac	ac		3	0
			ac		ac		2	0
				ac	ac		2	0
		me1		ac	ac		2	1
				ac			1	0
					ac		1	0
					ac	me1	1	1
		me1			ac		1	1
			me1		ac		1	1
		me1					0	1
			me1				0	1
				me1			0	1
							0	0

Table S3. H3K27 isoforms identified after propionylation of a nuclear extract from KARPAS-422 cells. Discrimination between methylation on K36 and K37 could not be always made and therefore in these cases both isoforms are reported.

Peptide H3 27-40 KSAPATGGVKKPHR

K27	K36	K37
me3		
me1	me2	
me1	me2	
me2	me1	
ac	me1	
	me1	
me1		
me1	me1	
me2	ac	me2
me2	me2	ac
me2	me2	
	ac	me2
	me2	ac
ac	me2	
me3	me2	
me1	ac	me2
me1	me2	ac
me2		
	me2	
ac		

Table S4. Precursor and fragment ion masses used in assay data

Figure 3 – peak areas of the extracted ion current for the 2+ and 3+ precursors were summed.

	Precursor	Precursor	Fragment	Fragment	Fragment	Fragment
unmethylated	480.2757 (3+)	719.9099 (2+)				
monomethylated	599.0023 (3+)	897.9989 (2+)				
dimethylated	603.6746 (3+)	905.0070 (2+)				

Figure 5 – peak areas of the extracted ion current for b-35 and b-45 fragment ions were summed.

	Precursor	Fragment	Fragment	Fragment	Fragment	
SDMA	603.6746 (3+)	383.1675 b4-31	553.2730 b5-31	610.2944 b6-31		
ADMA	603.6746 (3+)	397.1831 b4-45	567.2886 b5-45	624.3100 b6-45		

Figure 7 – peak areas of the extracted ion current for the 2+ and 3+ precursors were summed

	Precursor (2+)	Precursor (3+)	Fragment	Fragment	Fragment	Fragment
zero mods	520.6244	780.4344				
me	525.2985	787.444				
2 me	529.9701	794.4507				
me2	515.9669	773.4472				
me3	520.6395	780.4535				
me, me2	520.6395	780.4535				
2 me2	511.3076	766.4566				
me, me3	525.3119	787.4608				
me2, me3	515.979	773.4636				

Figure S1. Reverse phase chromatography of histone tryptic peptides after A) acetylation (top) or propionylation (bottom). Base peak LC-MS/MS chromatogram of a tryptic digest from the nuclear prep of Z138 cells. The same amount of tryptic digest is injected in both cases; B) accurate mass (+/- 10 ppm) extracted ion chromatograms for the precursor (2+, 3+) of select H3.1 peptides from these two analyses. The H3.1 18-26 peptide (top) with no modifications shows no difference in peak width or sensitivity after derivatization with either acetic or propionic anhydride. Chromatography of the acetylated or propionylated H3.1 27-40 peptides (bottom) shows comparable resolution for a similar set of modifications.

A

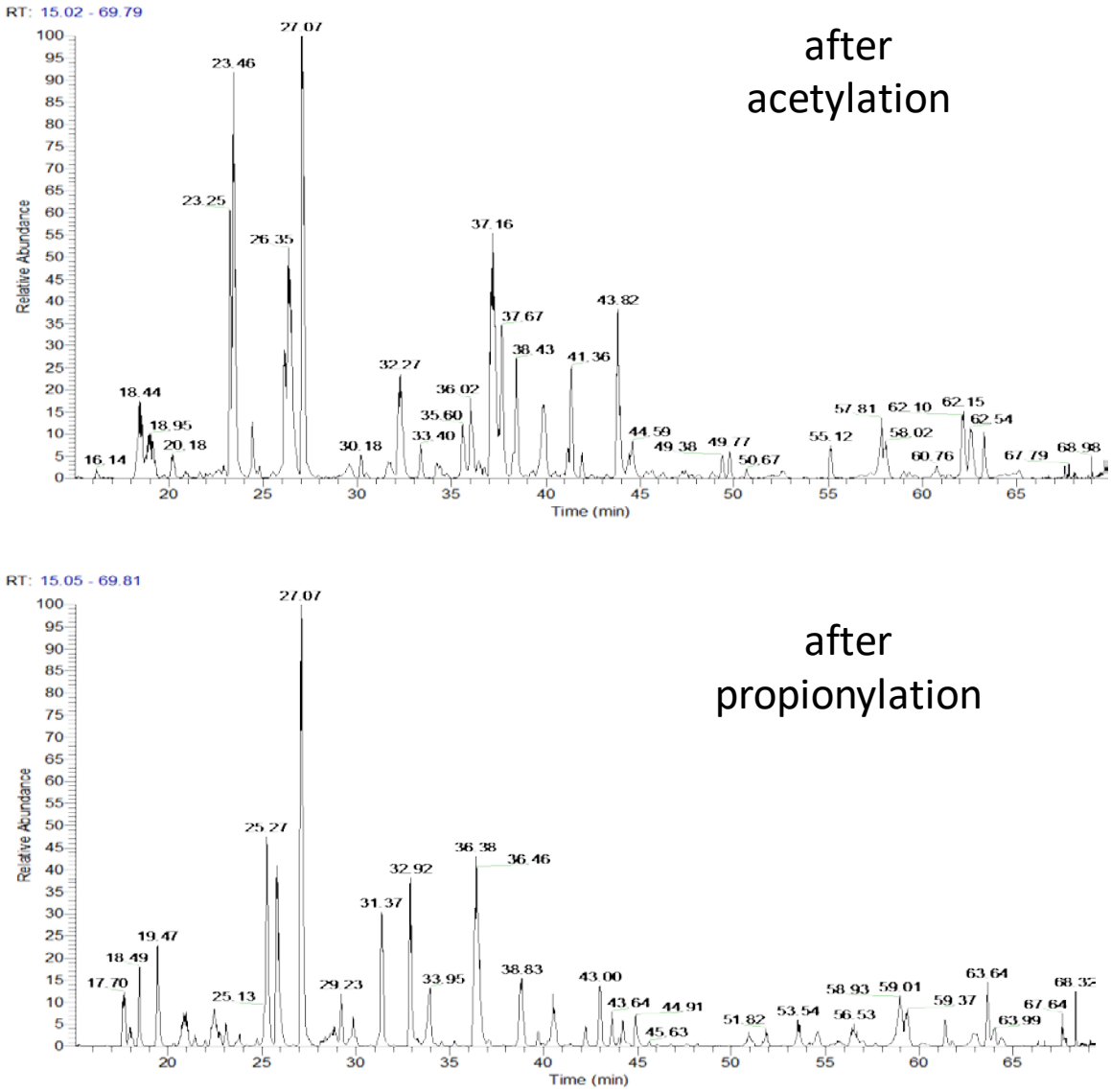

B

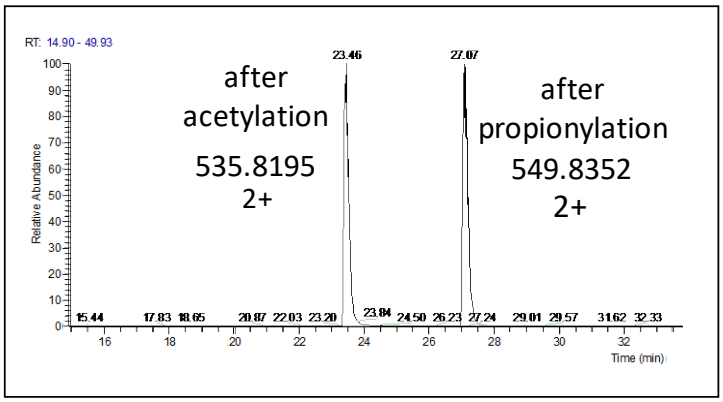

18 26
KQLATKAAR

no mods } 2Pr ⟶ 1083.6400

no mods } 2Ac ⟶ 1069.6243

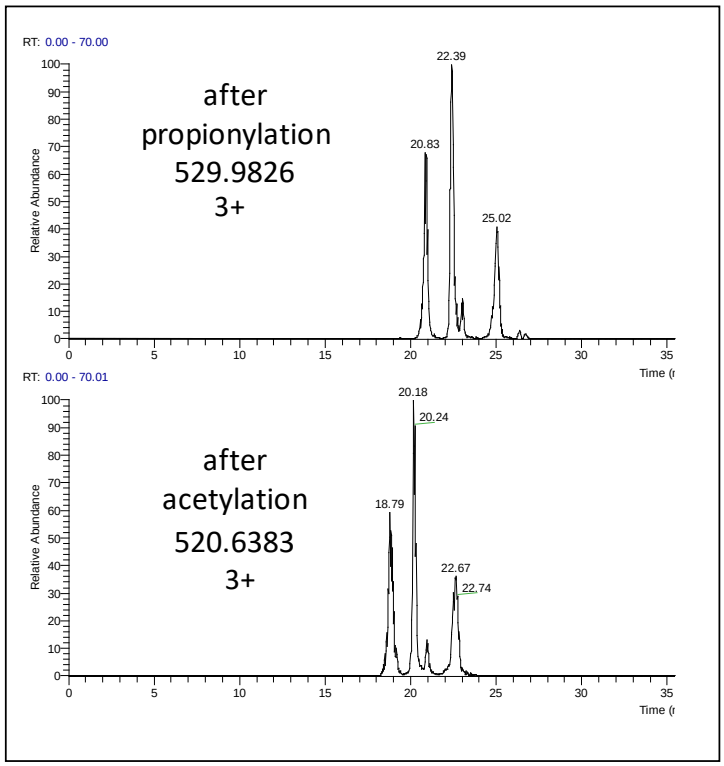

27 40
KSAPATGGVKKAHR

Me, Me2 } Bu, Me2, Pr
Me3 } Me3, 2Pr
Me3, Me, Ac } Me3, Bu, Ac
Ac } Ac, 2Pr
} 1586.9288

Me, Me2 } Pr, Me2, Ac
Me, Me2, Ac
Me3
Me3, Ac } Me3, 2Ac
Me3, 2Ac
} 1558.8943
No mods } 3Ac

In general we assume that in the case of derivatization with propionic anhydride, a butyl mark equals monomethyl plus propionyl and for derivatization with acetic anhydride, that a propionyl mark equals monomethyl plus acetylation. In the cases reported here, this has been validated by labeling with deuterated reagents.

Figure S2. (A) Schematic showing the acetylation and tryptic digestion of a 1:1:0.5:0.5 mixture of Histone H4R3 0MA:MMA:DMA synthetic peptide standards. (B) A 10-point 5-fold serial dilution was generated from 10pmol/µL to 5.12amol/µL in a 50ng/µL HeLa digest background. Full scan MS data for 3 technical replicate injections of each sample were acquired. Peak areas of $[M+2H]^{2+}$ + $[M+3H]^{3+}$ precursor ions for H4R3 (4-17) 0MA, (1-17) MMA and (1-17) DMA were generated by integrating extracted ion chromatograms (XIC). Average peak area values plotted vs fmols on column (log_{10} scale) indicate a linear response for all three components across the range of peak areas observed for the endogenous H4R3 peptides in the MDA-MB-468 nuclear preparations. These data were used to generate MS response correction factors of 1:3.0:0.9 for 0MA, MMA and DMA respectively.

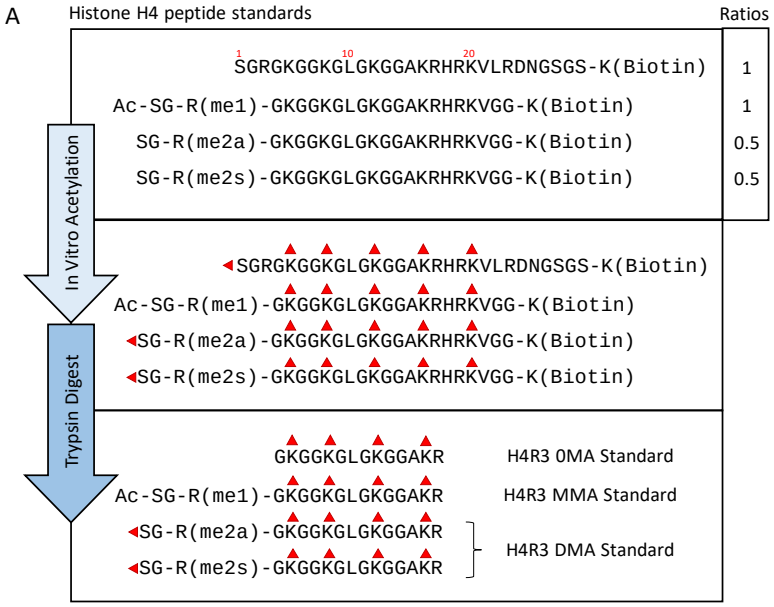

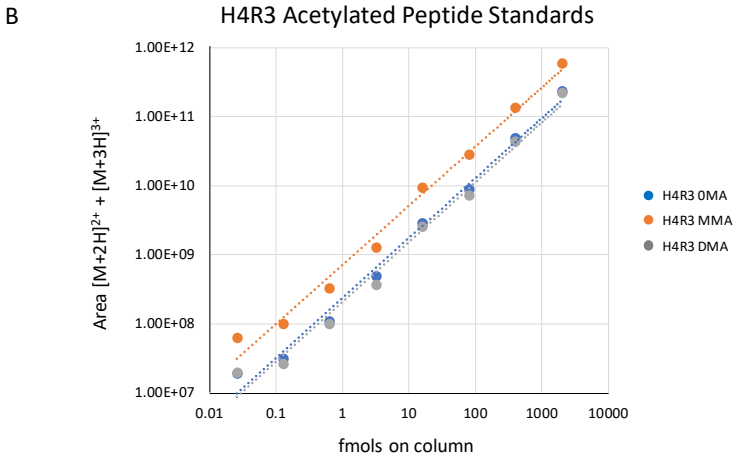

Figure S3: Optimization of the Normalized Collision Energy (NCE) for ADMA and SDMA neutral loss from H4R3 1-17 ADMA and SDMA peptides. In each case the precursor is the 3+ ion at m/z 603.6746. A) the NCE was ramped from 20 to 60 in increments of 2 and the response of the neutral loss from the b4-b6 ion series was monitored. B) MS/MS spectra for the fully acetylated synthetic H4 1-17 ADMA and C) SDMA peptides. Diagnostic ADMA and SDMA b ions are indicated.

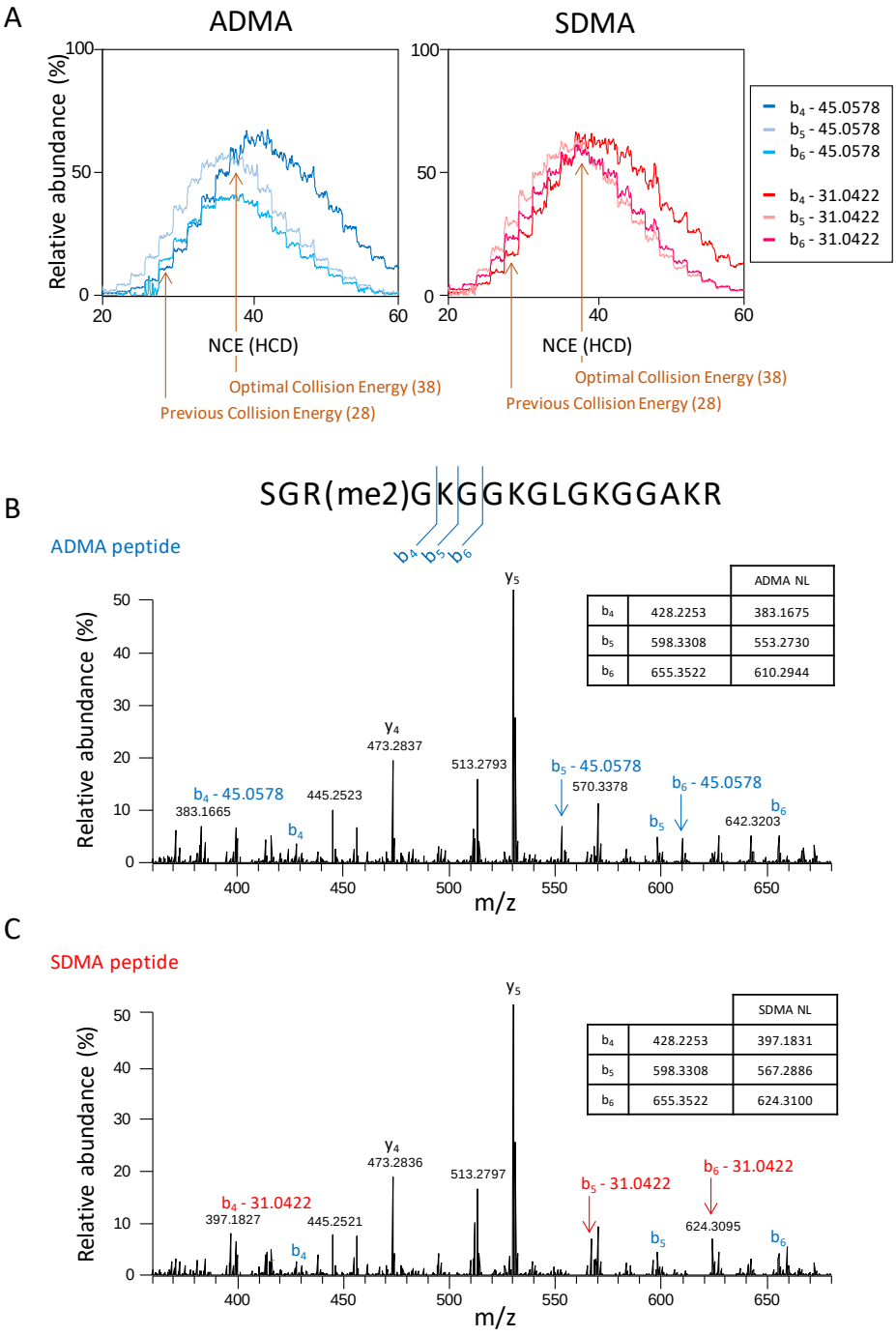

Figure S4: Discrimination of H4R3me2 ADMA from SDMA on the histone H4 1-17 peptide by tandem mass spectrometry. In each case the precursor is the 3+ ion at m/z 603.6746. The presence of either a 31.0422 Da (center) or 45.0578 Da (right) neutral loss from the b_4-b_6 ions (left) allows the unequivocal identification of H4R3 ADMA and SDMA.

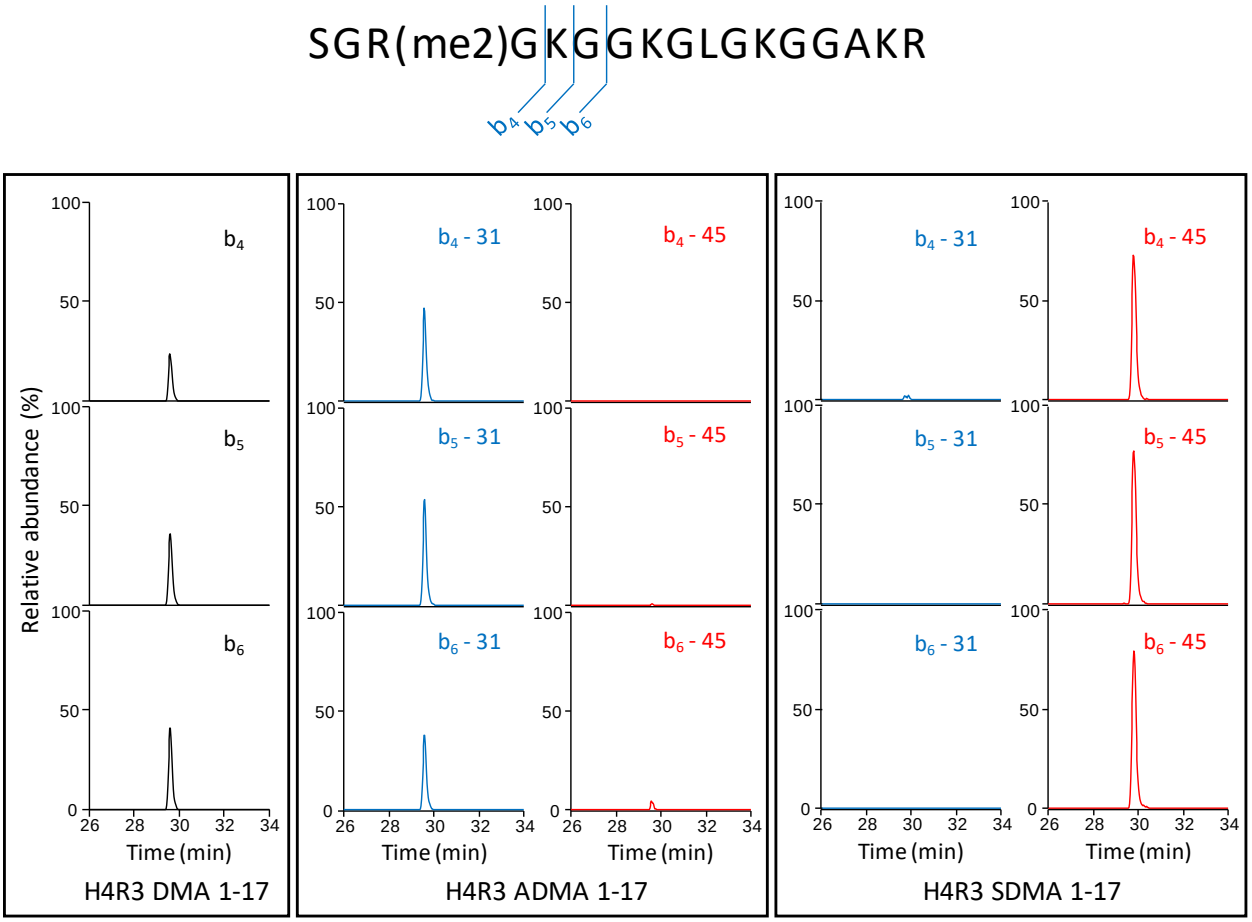

Figure S5. Tandem MS spectra representing species used in Figure 5. A) H4R3 zero, mono and dimethylarginine; B) H4R3 ADMA and SDMA

A

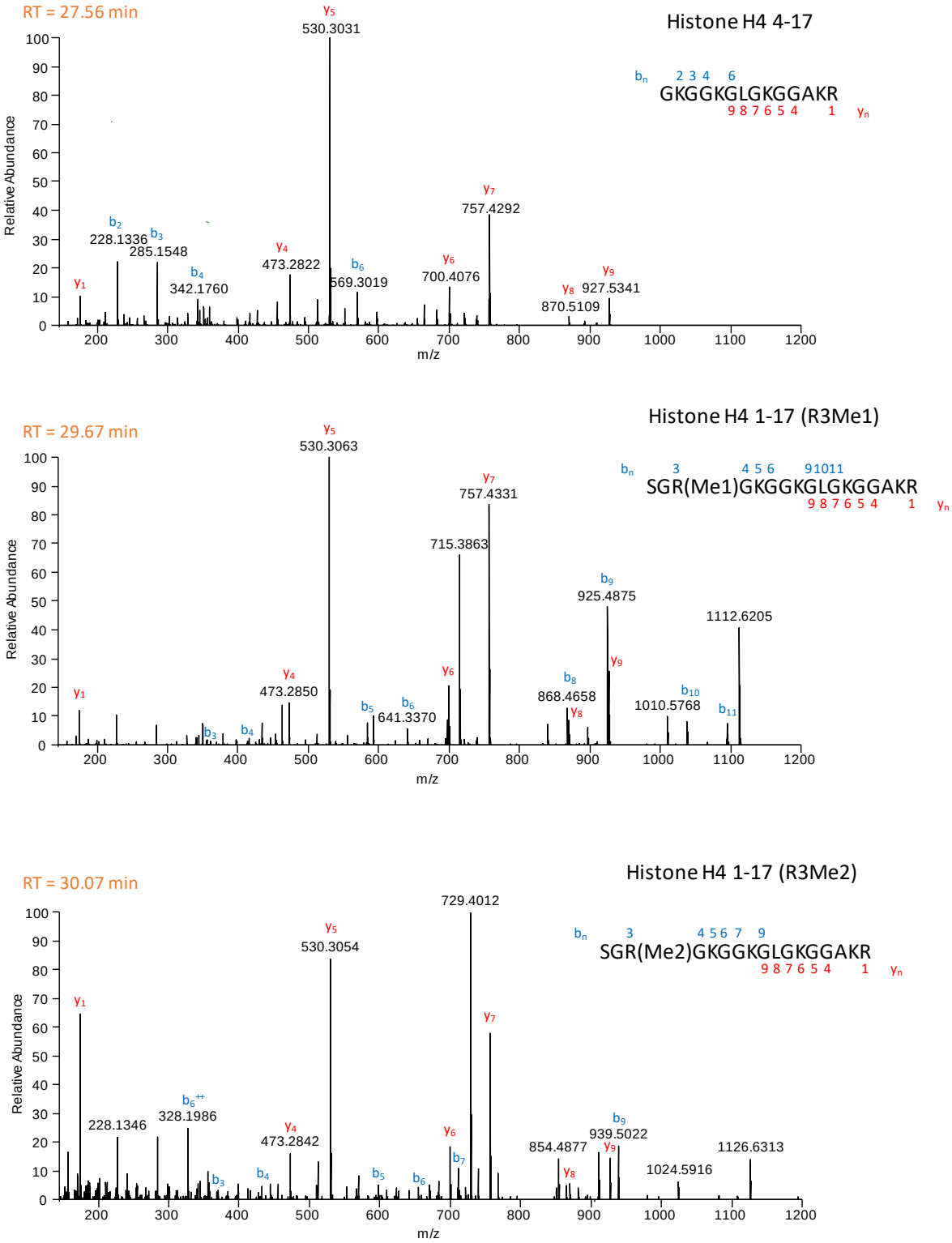

B

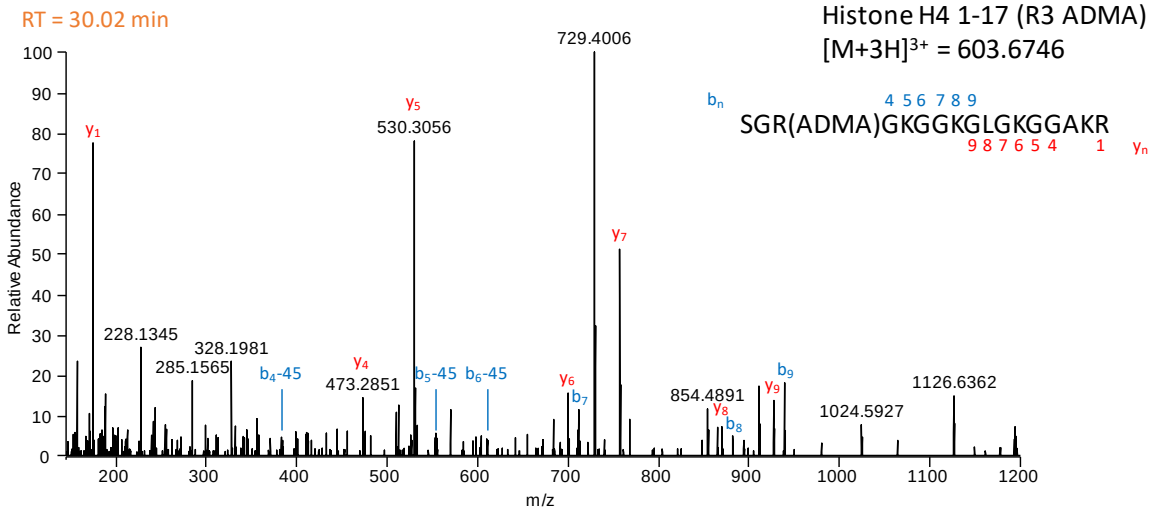
RT = 30.02 min
Histone H4 1-17 (R3 ADMA)
[M+3H]3+ = 603.6746
SGR(ADMA)GKGGKGLGKGGAKR
Relative Abundance
m/z
729.4006
530.3056
228.1345
328.1981
285.1565
473.2851
854.4891
1126.6362
1024.5927

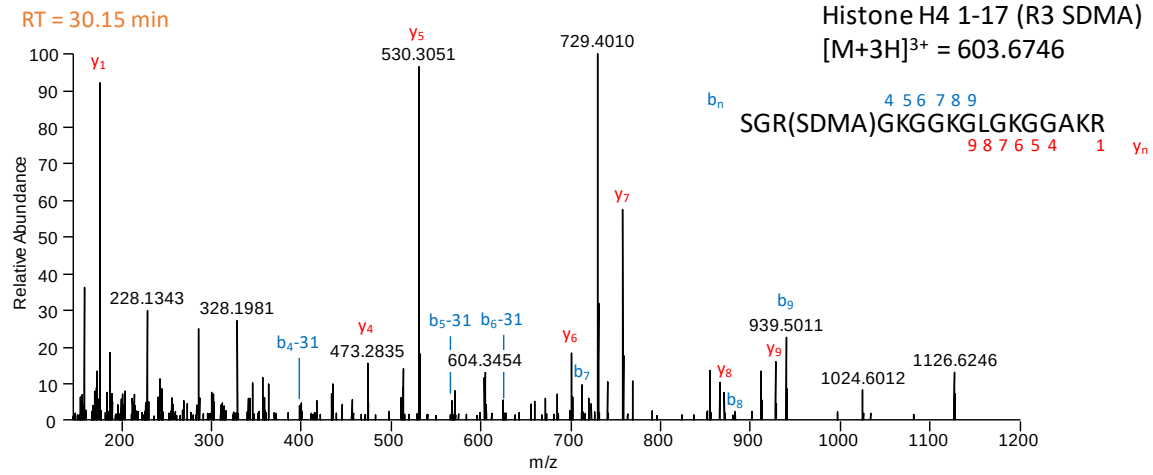
RT = 30.15 min
Histone H4 1-17 (R3 SDMA)
[M+3H]3+ = 603.6746
SGR(SDMA)GKGGKGLGKGGAKR
Relative Abundance
m/z
729.4010
530.3051
228.1343
328.1981
473.2835
604.3454
939.5011
1126.6246
1024.6012

Figure S6. (A) Extracted ion chromatograms from the PRM analysis of m/z 726.9178, the $[M+2H]^{2+}$ precursor ion for the tryptic peptide H4 (4-17) + me1. The sequence contains four lysine that can be methylated, K5, K8, K12 and K16. These ion profiles, diagnostic for methylation at the different lysine suggest multiple monomethyl species. The peak at RT 28.49 (A, black trace) has a spectrum (C, top) with a y_5 ion at m/z 530.3048 that confirms there is no methylation on K16. The y_6+14 ion at m/z 714.4268 confirms methylation on K12. All subsequent y ions, up to y_{12}, show evidence of methylation. This suggests this peak is primarily a single species methylated at K12. The peak with a RT 28.32 (A, red trace) has a spectrum (C, bottom) that shows a mixed population for ions y_5-y_{12} bearing 0 and 1 methyl group. The presence of a y_5+14 ion at m/z 544.3232 clearly indicates that part of this population has methylation on K16. However, the extracted ion chromatogram for m/z 544.3232 (A, green trace) places it on the right shoulder of the 28.32 peak. The left shoulder of this peak is characterized by unmethylated y_5 ions up to y_{12}, suggesting that part of the population is primarily K5me1. While it is possible that the peak contains some K8me1, the unchanging ratio of y and y+14 ions in the spectrum from y_5 to y_{12}, suggests that the y+14 ions come from the overlap of the K16me1 species that nearly co-elutes.

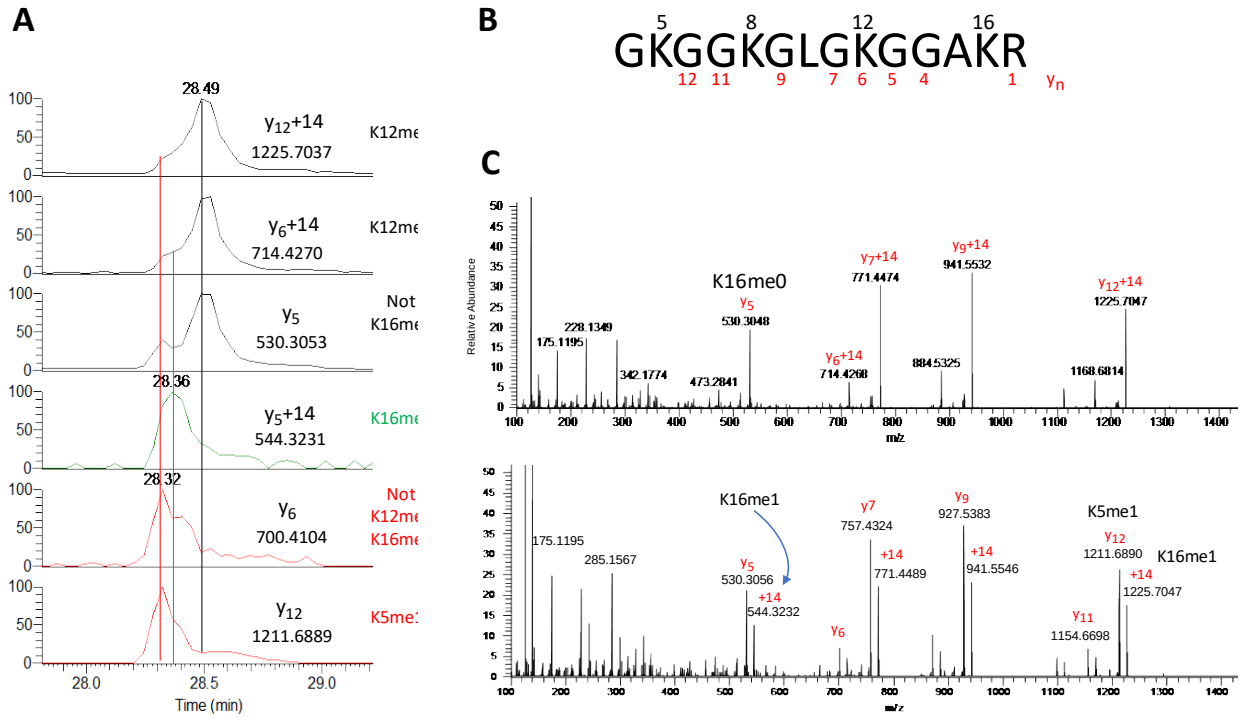

Figure S7. Tandem MS spectra for species represented in Figure 7.

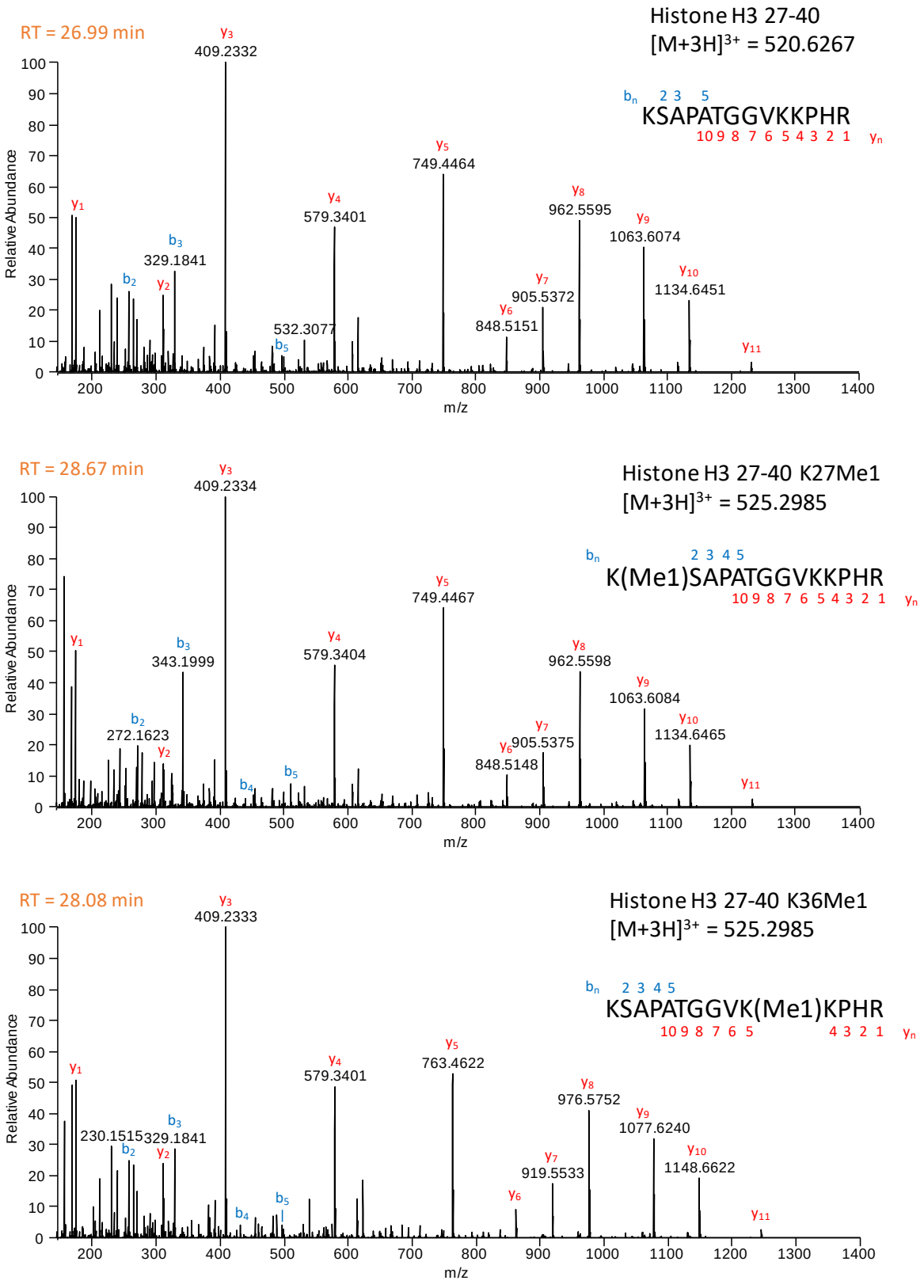

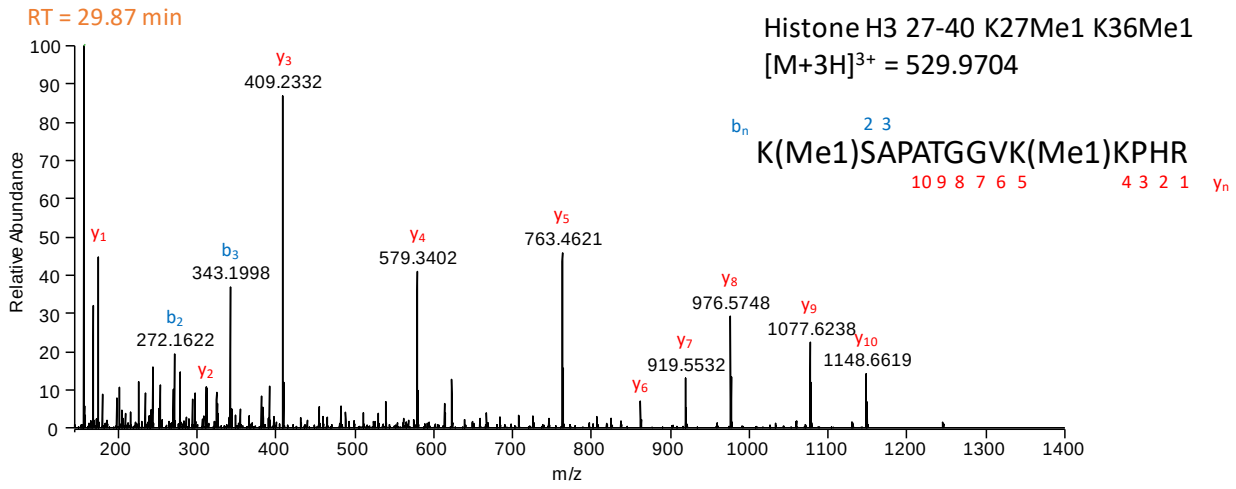
RT = 29.87 min
Histone H3 27-40 K27Me1 K36Me1
[M+3H]3+ = 529.9704
bn 2 3
K(Me1)SAPATGGVK(Me1)KPHR
10 9 8 7 6 5 4 3 2 1 yn
Relative Abundance
m/z
y3 409.2332
y1
b3 343.1998
y4 579.3402
y5 763.4621
b2 272.1622
y2
y8 976.5748
y9 1077.6238
y7 919.5532
y10 1148.6619
y6

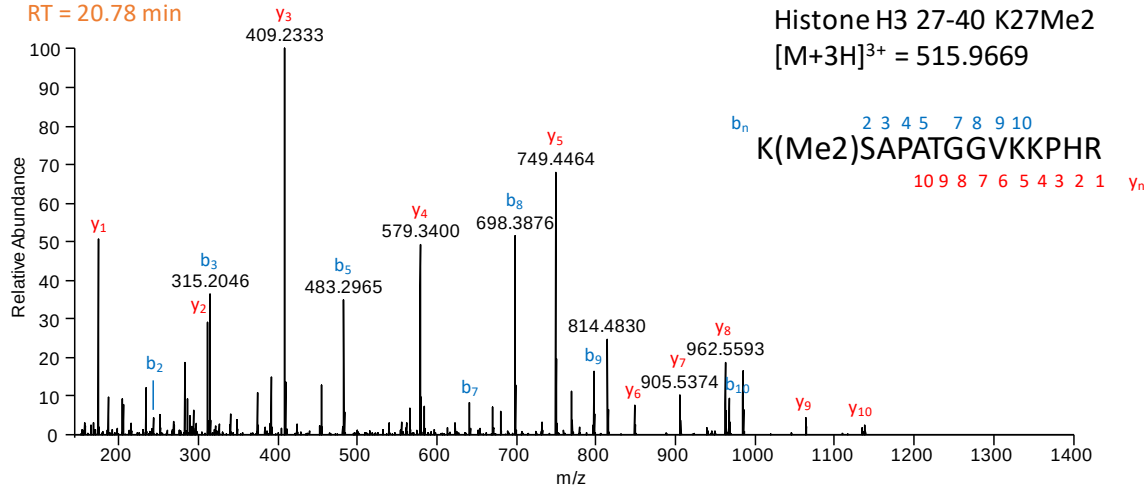
RT = 20.78 min
Histone H3 27-40 K27Me2
[M+3H]3+ = 515.9669
bn 2 3 4 5 7 8 9 10
K(Me2)SAPATGGVKKPHR
10 9 8 7 6 5 4 3 2 1 yn
Relative Abundance
m/z
y3 409.2333
y5 749.4464
y1
b8 698.3876
y4 579.3400
b3 315.2046
b5 483.2965
y2
814.4830
y8 962.5593
b2
b9
y7 905.5374
b7
y6
b10
y9
y10

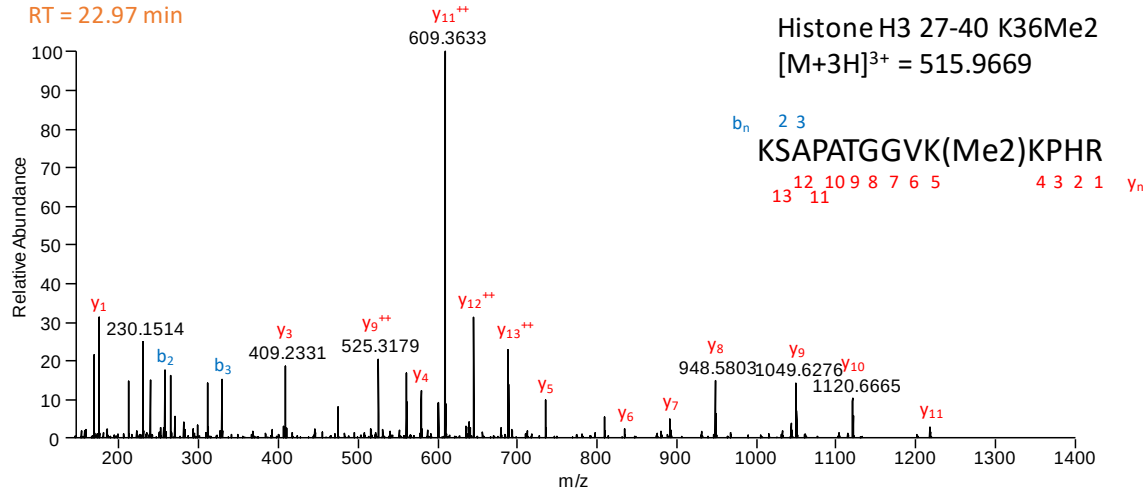
RT = 22.97 min
Histone H3 27-40 K36Me2
[M+3H]3+ = 515.9669
bn 2 3
KSAPATGGVK(Me2)KPHR
13 12 11 10 9 8 7 6 5 4 3 2 1 yn
Relative Abundance
m/z
y11++ 609.3633
y1
230.1514
y12++
y3 409.2331
y9++ 525.3179
y13++
b2
b3
y4
y8 948.5803
y9 1049.6276
y10 1120.6665
y5
y6
y7
y11

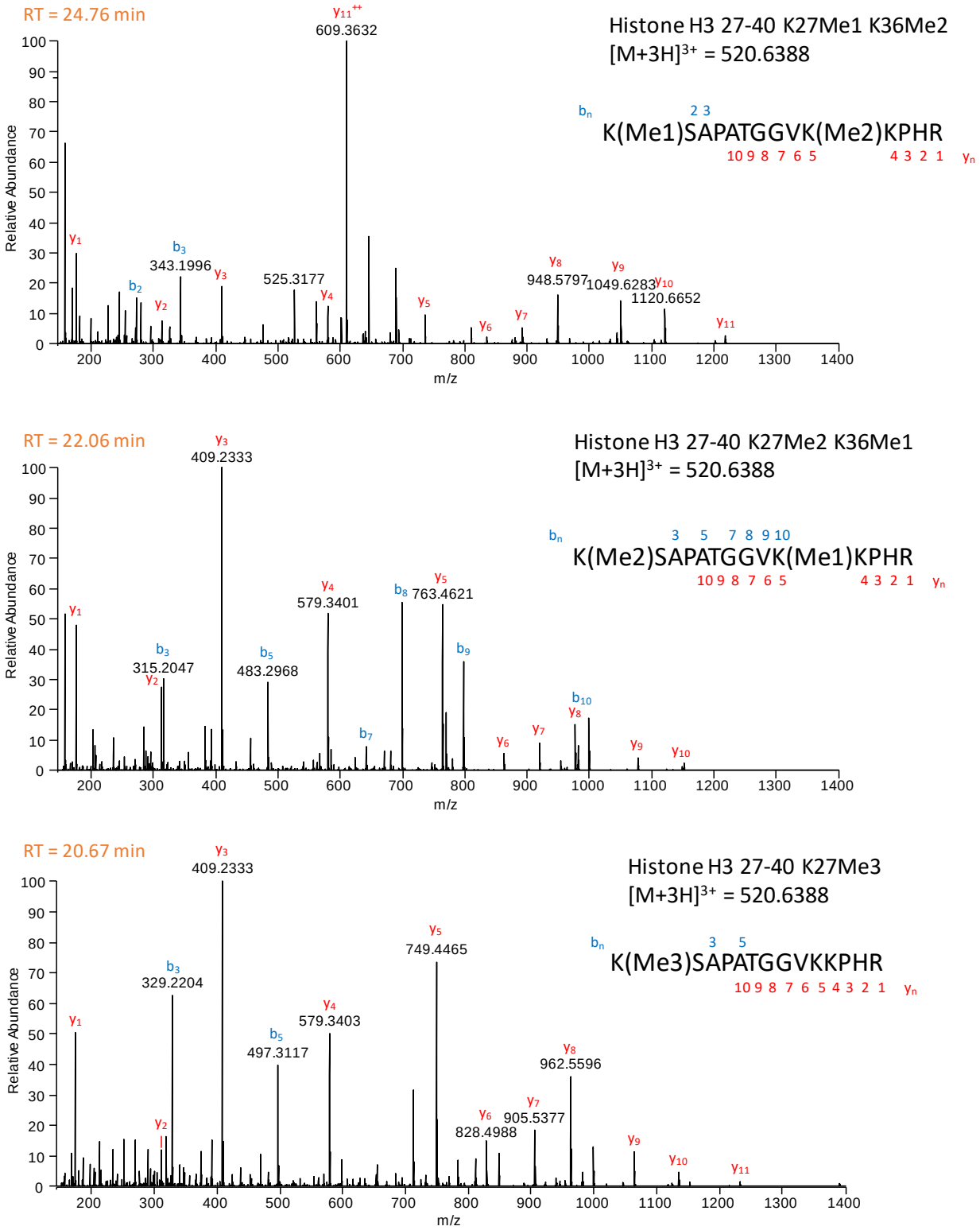
RT = 24.76 min
Histone H3 27-40 K27Me1 K36Me2
[M+3H]3+ = 520.6388
bn 2 3
K(Me1)SAPATGGVK(Me2)KPHR
10 9 8 7 6 5 4 3 2 1 yn
Relative Abundance
m/z
RT = 22.06 min
Histone H3 27-40 K27Me2 K36Me1
[M+3H]3+ = 520.6388
bn 3 5 7 8 9 10
K(Me2)SAPATGGVK(Me1)KPHR
10 9 8 7 6 5 4 3 2 1 yn
Relative Abundance
m/z
RT = 20.67 min
Histone H3 27-40 K27Me3
[M+3H]3+ = 520.6388
bn 3 5
K(Me3)SAPATGGVKKPHR
10 9 8 7 6 5 4 3 2 1 yn
Relative Abundance
m/z

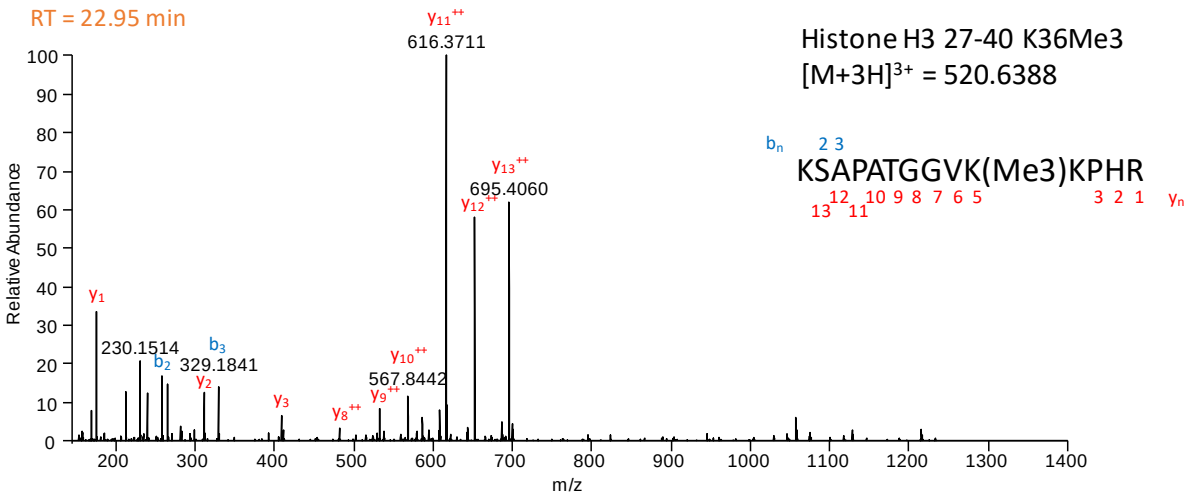
RT = 22.95 min
Histone H3 27-40 K36Me3
[M+3H]3+ = 520.6388
KSAPATGGVK(Me3)KPHR
616.3711
695.4060
567.8442
230.1514
329.1841
Relative Abundance
m/z

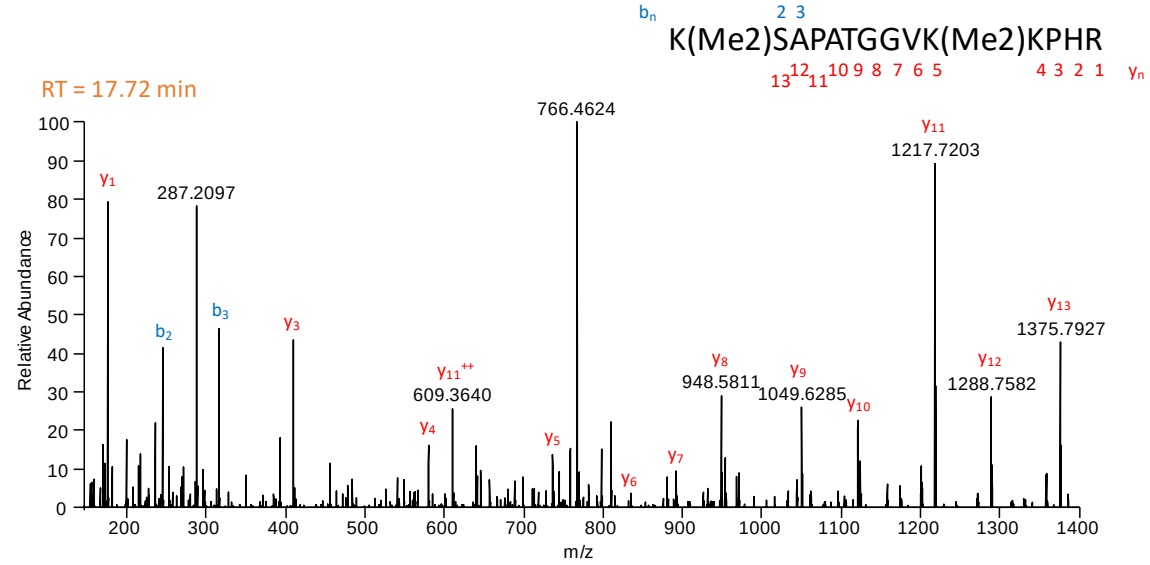
Histone H3 27-40 K27Me2 K36Me2
[M+2H]2+ = 766.4570
K(Me2)SAPATGGVK(Me2)KPHR
RT = 17.72 min
766.4624
1217.7203
287.2097
1375.7927
609.3640
948.5811
1049.6285
1288.7582
Relative Abundance
m/z

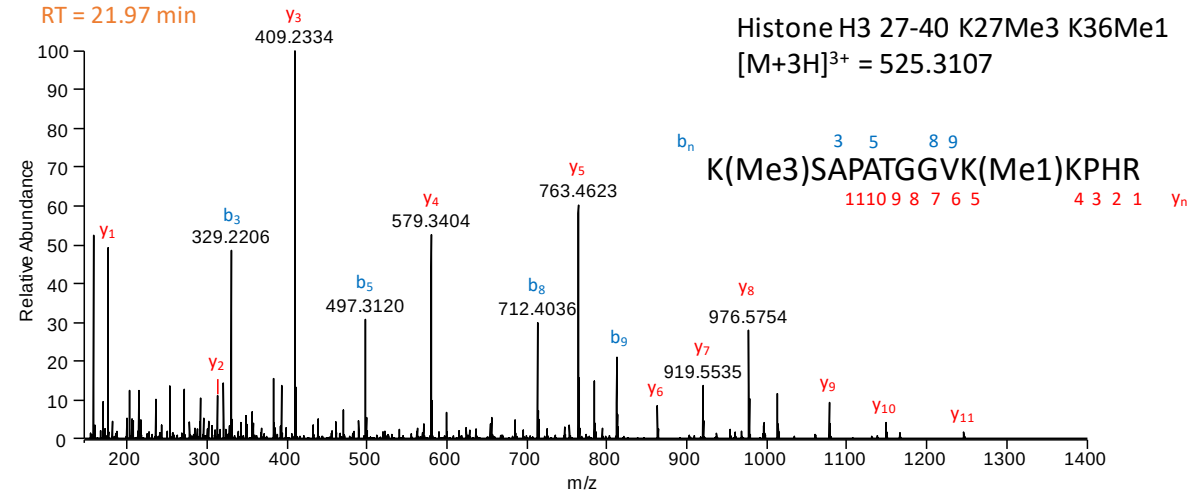
RT = 21.97 min
Histone H3 27-40 K27Me3 K36Me1
[M+3H]3+ = 525.3107
K(me3)SAPATGGVK(Me1)KPHR
409.2334
763.4623
579.3404
329.2206
497.3120
712.4036
976.5754
919.5535
Relative Abundance
m/z

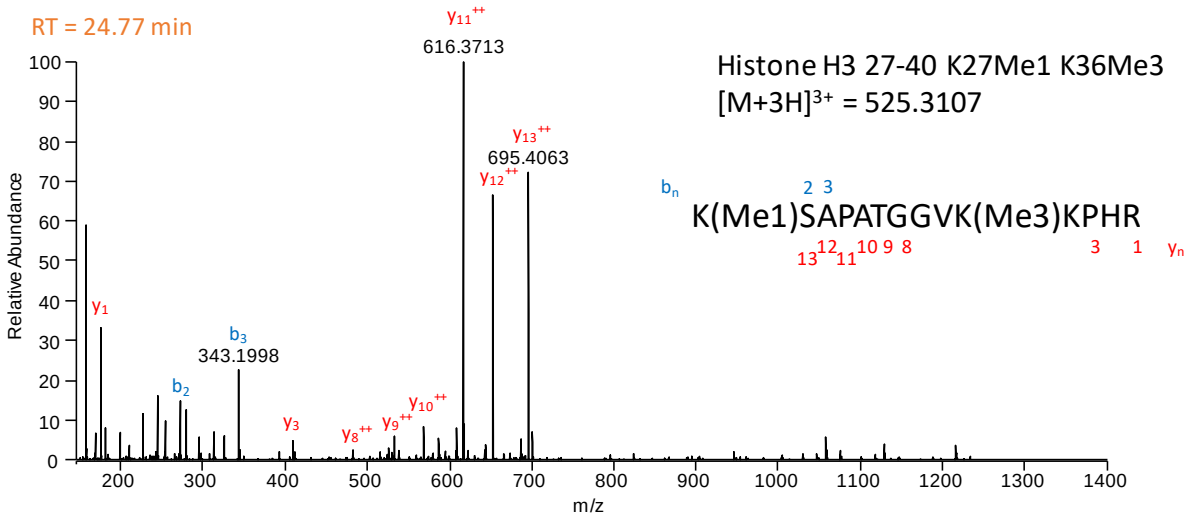
RT = 24.77 min
Histone H3 27-40 K27Me1 K36Me3
[M+3H]3+ = 525.3107
bn
2 3
K(Me1)SAPATGGVK(Me3)KPHR
13 12 11 10 9 8
3 1 yn
y11++
616.3713
y13++
695.4063
y12++
y1
b3
343.1998
b2
y3
y8++
y9++
y10++
Relative Abundance
m/z

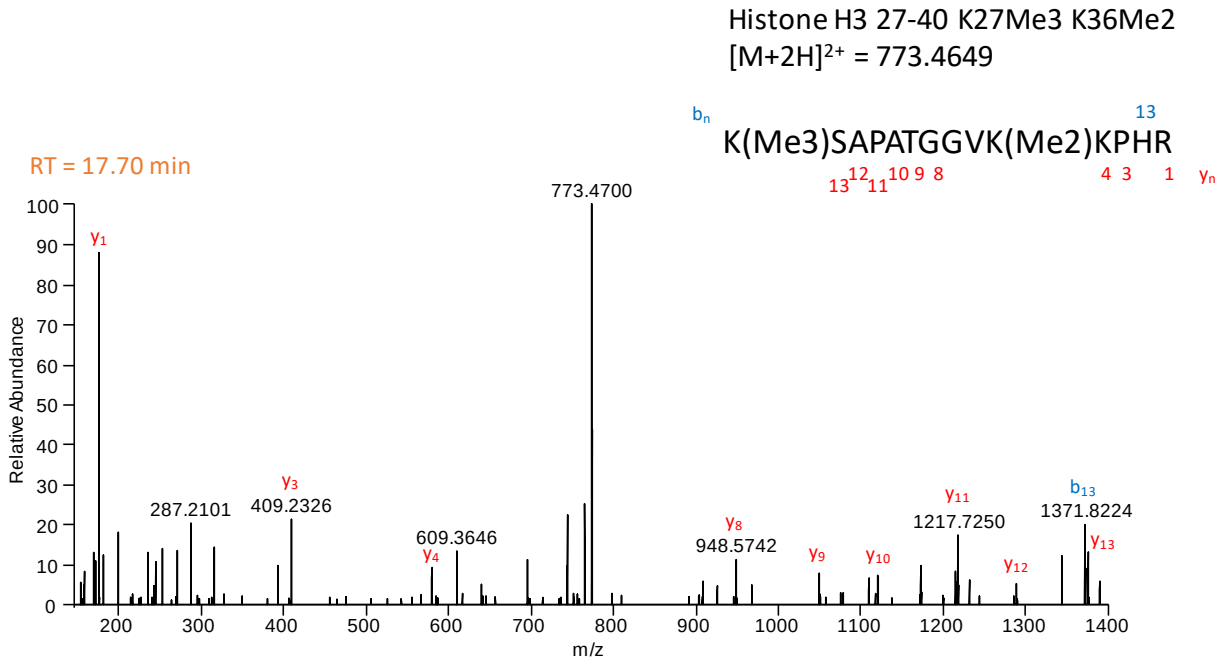
Histone H3 27-40 K27Me3 K36Me2
[M+2H]2+ = 773.4649
bn
13
K(Me3)SAPATGGVK(Me2)KPHR
13 12 11 10 9 8
4 3 1 yn
RT = 17.70 min
773.4700
y1
y3
409.2326
287.2101
609.3646
y4
y8
948.5742
y9
y10
y11
1217.7250
y12
b13
1371.8224
y13
Relative Abundance
m/z